

## High-pressure-induced phase transitions of mercury chalcogenides

Tzuen-Luh Huang and Arthur L. Ruoff

*Department of Materials Science and Engineering, Cornell University, Ithaca, New York 14853*

(Received 27 July 1984)

The high-pressure-induced phase transitions of mercury chalcogenides (including sulfide, selenide, and telluride) were studied to 40 GPa using energy-dispersive x-ray diffraction with a diamond anvil cell. The common pressure-induced transition sequence in these compounds was found to be zinc blende (phase I), cinnabar (phase II), NaCl (phase III), and body-centered tetragonal (phase IV). Relative intensity measurements were compared to relative intensity calculations to determine the space groups of phases III and IV. Another high-pressure phase (phase V) of HgTe was found. The high-pressure phase-transition sequence of mercury chalcogenides is similar to that for the zinc and cadmium chalcogenides except for the intermediate cinnabar phase in the mercury chalcogenides.

### I. INTRODUCTION

Since the early work of Drickamer *et al.* on the resistance discontinuity of IIB-VI and III-V compounds as a function of pressure,<sup>1,2</sup> many efforts have been made to identify the crystal-structural transitions corresponding to these resistance changes.<sup>3-7</sup> It has been suggested that most IIB-VI compounds, which have either the zincblende or wurtzite crystal structure (both are fourfold coordinated) at atmospheric pressure, will transform to the NaCl crystal structure (sixfold coordinated) under high pressure.<sup>8</sup> Zinc and cadmium compounds have been shown to undergo this kind of transition<sup>3-7</sup> while only a few studies had been done on mercury chalcogenides<sup>9,10</sup> when the present study was undertaken. Because Zn, Cd, and Hg have a similar valence electronic configuration  $(n-1)d^{10}ns^2$ , they have similar bonding (covalent  $sp^3$  bonding) and similar crystal structure at atmospheric pressure. The mercury chalcogenides differ from the other two chalcogenides in two ways. First, HgSe and HgTe are semimetals instead of semiconductors at atmospheric pressure despite the  $sp^3$  bonding. Second, HgS has a metastable zinc-blende phase at atmospheric pressure while the cinnabar structure is the stable phase. Both zinc-blende phases of HgSe and HgTe transform into the cinnabar structure at very low pressures,<sup>9-11</sup> while no such transition is observed in the zinc and cadmium chalcogenides.

These mercury compounds when alloyed with Cd are the so-called narrow band-gap semiconductors used as infrared detector materials<sup>12</sup> and the resistivity measurement as a function of pressure on HgTe (Ref. 11) shows that it undergoes the transition from semimetal to semiconductor to metal in a relatively narrow pressure range. These resistivity changes are also accompanied by crystal structural transitions from the zinc blende (phase I) to the cinnabar (phase II) to the NaCl (phase III, tentatively indexed earlier) to an unknown crystal structure (phase IV). We have previously reported the high-pressure x-ray diffraction studies of HgS (to 40 GPa),<sup>13</sup> HgSe (to 40 GPa),<sup>14</sup> and HgTe (to 15.0 GPa).<sup>15</sup> The unknown phase IV was tentatively indexed (without relative intensity considera-

tions) as possibly being an orthorhombic crystal structure. Concurrent independent diffraction studies by Werner *et al.* on HgTe and HgS to 20 GPa (Ref. 16) showed that the phase IV of HgTe has a  $\beta$ -Sn crystal structure.

Werner *et al.*<sup>16</sup> also reported Raman scattering studies on HgS. It is expected that these lines should disappear completely if an NaCl structure is formed. Inasmuch as all of these lines did not disappear they assumed that the NaCl structure had not formed at 20 GPa. In all these studies, no efforts have been made to determine the space group of the high-pressure phase (for which intensity measurements must be available) although the usage of the terminology such as the NaCl and the  $\beta$ -Sn structure implied the space group of the high-pressure phase. In this report, we summarize the previous results on the high-pressure-induced phase transitions of these three compounds and carry out the relative intensity calculations of the diffraction pattern to confirm the space group of the high-pressure phases. Moreover, we extend the x-ray diffraction study of HgTe to 40 GPa and observe another new crystal structural transition (phase IV to phase V). These experimental results shed light on the understanding of the high-pressure-induced structural transitions of the other IIB-VI compounds (zinc and cadmium chalcogenides) which have a similar bonding and crystal structure and provide experimental results for the theoretical first-principles pseudopotential band structure and total-energy calculations.

### II. THEORY

Under very high pressure, a relatively open crystal structure may eventually collapse and transform to another crystal structure. Several different theories have been proposed to predict and explain these pressure-induced phase transitions, but at present all of them have limitations.

At first, one can find a clue to the phase transition sequence by looking at the crystal structure of the other compounds that have similar electronic structures at atmospheric pressure. For example from the third row of the Periodic Table (excluding the transition metal ele-

ments) and the  $AB$  compounds they form, one finds that element Ge has a diamond structure and is a semiconductor. The III-V compound GaAs and the IIB-VI compound ZnSe have a zinc-blende structure. The compounds CaSe and KBr have the NaCl structure. Note that the average atomic numbers of these compounds are the same. When a covalent bonded crystal (diamond or zinc-blende structure) is subjected to high pressure, the ion cores interact more strongly with the  $sp^3$  orbitals and the directional  $sp^3$  orbitals become more diffuse and ionic (NaCl structure).<sup>17</sup> One also notices that the solids of the group-IV elements, Si, Ge, and Sn, have a diamond structure while Sn also has a  $\beta$ -Sn structure which is a distorted NaCl structure<sup>18</sup> because the number of the first nearest neighbor is approximately 6. In the early days of high-pressure x-ray diffraction studies, this analogy was used as a guide to determine the high-pressure phase.

Based on the experimental results of high-pressure-induced phase transitions of IIB-VI and III-V compounds, Jayaraman *et al.*<sup>8</sup> proposed the high-pressure phase transition sequence for  $A^N B^{8-N}$  compounds. According to this theory, the sequence of polymorphic structures found with increasing pressure and/or atomic number reflecting increased coordination can be summarized as follows: graphite—wurtzite / diamond / zinc-blende— $\beta$ -Sn/NaCl—bcc/CsCl—closest packing. If the mean atomic number of these compounds is plotted versus electronegativity difference for different IIB-VI and III-V compounds, the whole area can be divided into metallic, intermediate, and ionic compound regions. Two boundary lines are drawn from the experimental results. Compounds falling into the metallic region will transform to the  $\beta$ -Sn structure upon becoming metallic. Compounds in the ionic region have the NaCl structure at atmospheric pressure and will transform to a metallic structure under high pressure. The mercury chalcogenides we are interested in fall into the intermediate region and very close to the boundary line.

A semiempirical theory was developed by Van Vechten.<sup>17</sup> He used a two-band model of semiconductor compounds and a free-electron model of metals to calculate the heat of fusion, melting point, and pressure-temperature phase diagrams of group-IV elements and III-V compounds; he successfully predicted the phase-transition pressures of some group-IV elements and III-V compounds. This theory is only good for the more covalent compounds, however, and his presumption that the new phase of these compounds would be the  $\beta$ -Sn crystal structure has not always proved to be true.<sup>19,20</sup>

Later, an *ab initio* pseudopotential approach to the total energy calculation was developed by Cohen and his co-workers.<sup>21</sup> A wide range of materials has been investigated with this approach, including insulators, semiconductors and metals. The calculated and experimental structural properties of these materials are in excellent agreement. Because it is impossible to do an exhaustive calculation on every possible structure, however, feedback from the experimental results of the high pressure structure is needed. It has also been found that for compounds, such as GaAs and GaP, the difference in the free energy of several structures is small.<sup>22</sup> This can be attributed to the limited reso-

lution of the calculation or it may also imply that several different phases may coexist under high pressure. Further studies are needed. Although this kind of calculation is still in its infancy, we hope that our experimental results can provide some guidance.

### III. EXPERIMENTAL METHODS

The details of the experimental methods were given by Baublitz *et al.*<sup>20</sup> High pressure was generated between two diamond flats of 640- $\mu\text{m}$  diameter. The Nimonic 80 A gasket was 150  $\mu\text{m}$  thick and had a hole of 150- $\mu\text{m}$  diameter. A methanol-ethanol 4:1 mixture was used as the pressure medium.<sup>23</sup> Ruby fluorescence was used as the pressure scale.<sup>24</sup> Energy dispersive diffraction with the Cornell High Energy Synchrotron Source (CHESS) was used. The typical data-collecting time was 20 min to 1 h. A figure of merit called the reliability factor  $R$ , is defined as follows:<sup>20</sup>

$$R = \sum_{hkl} \left| \frac{I_{\text{obs}}(hkl)}{\sum_{h'k'l'} I_{\text{obs}}(h'k'l')} - \frac{I_{\text{cal}}(hkl)}{\sum_{h''} I_{\text{cal}}(h''k''l'')} \right| \quad (1)$$

This is used to evaluate the fitness of the assigned crystal structure of the high-pressure phases.

### IV. EXPERIMENTAL RESULTS

#### A. HgTe

Figure 1 shows the diffraction pattern of HgTe at 8.9 GPa. The analysis of this diffraction pattern, given in Table I, shows that it has a NaCl structure; the reliability factor given by Eq. (1) is  $R=0.13$  where  $R=0$  represents perfect agreement. As the pressure increases, new diffraction peaks in addition to those from the NaCl structure start to appear at 12.0 GPa, but peaks of the NaCl structure (phase III) are still present. At 17.0 GPa, phase III completely disappears and the new diffraction pattern obtained (phase IV) (analysis given in Table II), is shown in Fig. 2. Details of the analysis of phase IV will be given later. The previously reported tentative orthorhombic crystal structure at 14.8 GPa (Ref. 15) is found to have been in fact a mixture of phase III and phase IV.

As we increased the pressure still further, a new diffrac-

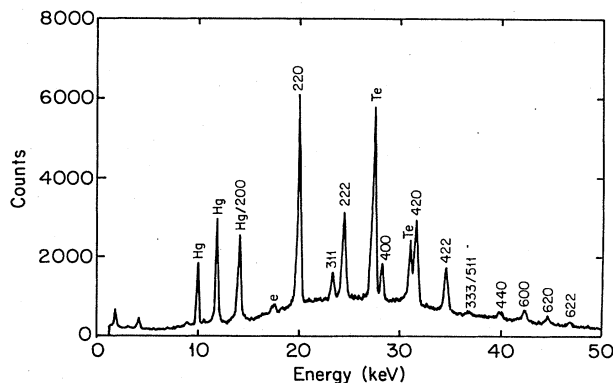


FIG. 1. Diffraction pattern of HgTe at 8.9 GPa.  $T=28^\circ\text{C}$ .

TABLE I. Analysis of the diffraction pattern of HgTe at 8.9 GPa, phase III, NaCl structure,  $a=5.843$  Å,  $\theta=8.642^\circ$ ,  $E_{\text{acc}}=5.0$  GeV,  $T=28^\circ\text{C}$ .

Index	$d_{\text{obs}}$	$d_{\text{cal}}$	$I_{\text{obs}}$	$I_{\text{cal}}$
200	2.925	2.922	29 <sup>a</sup>	21
220	2.067	2.066	100	100
311	1.761	1.762	11	9
222	1.686	1.687	48	43
400	1.461	1.461	13	18
420	1.306	1.307	22 <sup>b</sup>	42
422	1.193	1.193	26	21
333/511	1.124	1.124	3	1
440	1.032	1.033	4	4
600	0.974	0.974	5	1
620	0.923	0.924	3	4
622	0.880	0.880	2	3

<sup>a</sup>This peak coincides with the third Hg fluorescence peak whose intensity has been subtracted; hence anomalous absorptions may occur so this peak is excluded from the calculation of the reliability factor.

<sup>b</sup>This peak is close to the Te absorption edge where anomalous absorption occurs and is excluded in the calculation of the reliability factor. Here  $R=0.13$ .

TABLE II. Analysis of the diffraction pattern of HgTe at 17.0 GPa, phase IV, body-centered-tetragonal lattice,  $a=5.524$  Å,  $c=2.973$  Å,  $\theta=8.051^\circ$ ,  $E_{\text{acc}}=5.4$  GeV,  $T=28^\circ\text{C}$ .

Index	$d_{\text{exp}}$	$d_{\text{cal}}$	$I_{\text{obs}}$	$I_{\text{cal}}^a$	$I_{\text{cal}}^b$
200	2.762	2.762	13	30	38
101	2.618	2.618	66	39	36
220	1.896	1.953	147	147	147
211		1.900			
310	1.788	1.747	9	5	7
301	1.526	1.565	15	27	44
002		1.487		1	
112		1.389			
400	1.385	1.381	c	84	54
321		1.362			
202	1.314	1.309	33	3	34
330		1.302			
420	1.219	1.235	22	27	30
411		1.221			
222	1.184	1.183	11	1	17
440	0.948	0.977	2	3	3
422		0.950			

<sup>a</sup>Basis: Hg(0,0,0), Te  $(0, \frac{1}{2}, \frac{1}{4})$ .

<sup>b</sup>Basis: Hg(0,0,0), Te  $(0, \frac{1}{2}, 0)$ .

<sup>c</sup>This peak is close to the K absorption edge of Te and hence not included in the calculation of  $R$ . The reliability factors,  $R$ , are 0.46 and 0.33 for the two cases of a and b, respectively.

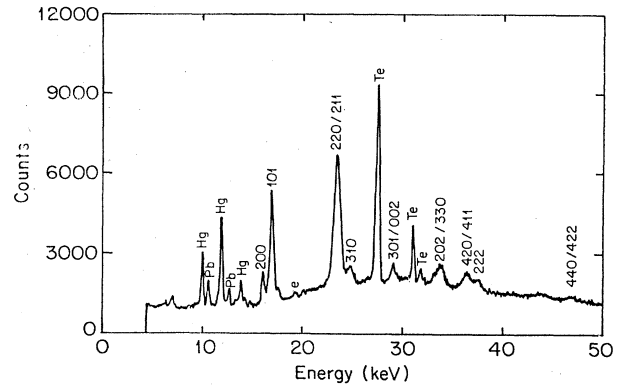


FIG. 2. Diffraction pattern of HgTe at 12.0 GPa.  $T=28^\circ\text{C}$ .

tion peak started to appear at 38.1 GPa. Figure 3 shows the diffraction pattern of HgTe at 41.0 GPa. In addition to the peaks which can be indexed as the NaCl structure, there were three extra peaks (labeled  $V1$ ,  $V2$ , and  $V3$  in Fig. 3) indicating the presence of phase V. The crystal structure of this new phase may be a distorted CsCl structure and will be discussed more in the next section.

### B. HgSe

The analysis of the diffraction pattern of HgSe at 20.9 GPa is listed in Table III. The  $d$  spacings fit the face-centered cubic lattice and the relative intensity calculation shows that it has a NaCl crystal structure; the reliability factor is  $R=0.10$ .

Figure 4 shows a series of diffraction patterns of HgSe between 28.0 and 40.4 GPa. As the pressure increases, new diffraction peaks in addition to those of the NaCl structure were observed. The intensities of the new diffraction peaks of the new phase increased at the expense of the low-pressure phase III (the NaCl phase). The analysis of the diffraction pattern of HgSe at 40.4 GPa is given in Table IV. Phase IV is proposed to have a body-centered-tetragonal (bct) structure possibly with a basis Hg(0,0,0) and Se  $(0, \frac{1}{2}, \frac{1}{4})$  or Hg(0,0,0) and Se  $(0, \frac{1}{2}, 0)$ . The previously reported tentative orthorhombic structure<sup>14</sup> has been discarded because the relative-intensity calculation of that model does not fit well with the observed intensities.

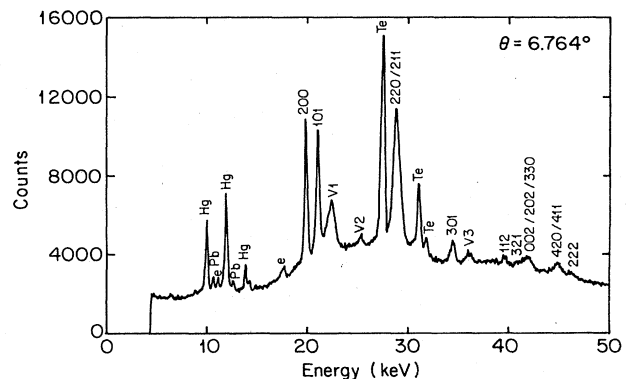


FIG. 3. Diffraction pattern of HgTe at 41.0 GPa.  $T=28^\circ\text{C}$ .

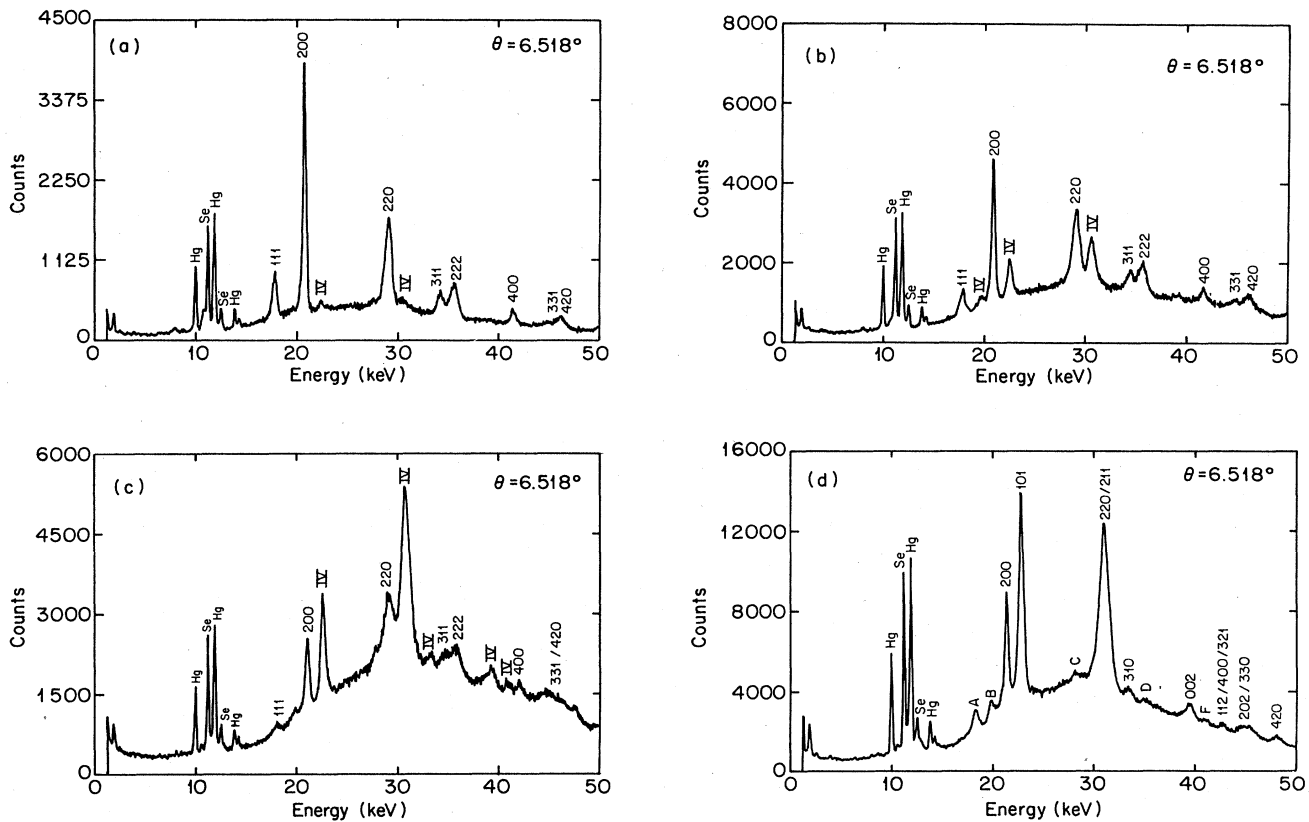


FIG. 4. (a) Diffraction pattern of HgSe.  $T=28^\circ\text{C}$ ,  $P=23.4$  GPa. (b) Diffraction pattern of HgSe.  $T=28^\circ\text{C}$ ,  $P=30.4$  GPa. (c) Diffraction pattern of HgSe.  $T=28^\circ\text{C}$ ,  $P=32.8$  GPa. (d) Diffraction pattern of HgSe.  $T=28^\circ\text{C}$ ,  $P=40.4$  GPa.

A detailed discussion of phase IV of HgSe is given in the next section.

### C. HgS

Figure 5 shows the diffraction pattern of the cinnabar structure of HgS at atmospheric pressure. As the pressure was increased, the (110), (111), and (104) peaks which were overlapping but resolvable, shifted closer to one another and became a single peak at about 13 GPa, which can be indexed as the (220) peak of the NaCl structure. At the same time, the (201), (113), and (105) peaks became a doublet peak which can be indexed as the (311) and

(222) peaks of the NaCl phase. The diffraction pattern obtained at 30 GPa has been indexed as a NaCl structure<sup>13</sup> with a reliability factor of  $R=0.16$  ( $R=0$  represents perfect fit). No further phase transition was observed to 40 GPa.

### V. DISCUSSION

In the study of HgS to 20 GPa, Werner *et al.*<sup>16</sup> found that the (101) and (003) diffraction peaks of the cinnabar phase merge with increasing pressure and cannot be

TABLE III. Analysis of the diffraction pattern of HgSe at 21.0 GPa, phase III, NaCl structure,  $a=5.360$  Å,  $\theta=6.518^\circ$ ,  $E_{\text{acc}}=5.0$  GeV,  $T=28^\circ\text{C}$ , reliability factor  $R=0.10$ .

Index	$d_{\text{obs}}$	$d_{\text{cal}}$	$I_{\text{obs}}$	$I_{\text{cal}}$
111	3.102	3.095	9	5
200	2.677	2.680	70	63
220	1.897	1.895	100	100
311	1.617	1.616	21	21
222	1.547	1.547	34	29
400	1.339	1.340	13	9
331	1.229	1.230	9	4
420	1.198	1.198	18	17

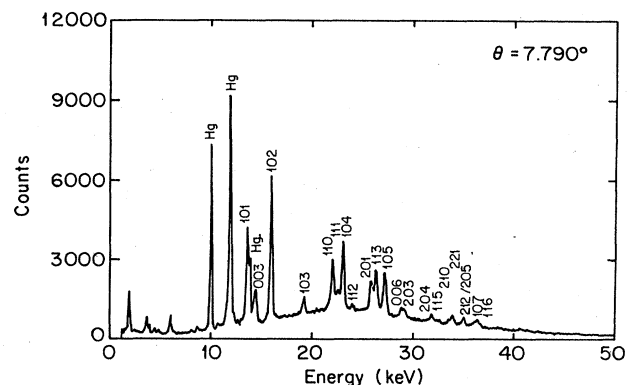


FIG. 5. Diffraction pattern of HgS.  $T=28^\circ\text{C}$ ,  $P=300$  kbar.

separated above 10 GPa; this is lower than 13 GPa reported here. This disagreement is probably due to the difference in the resolution of the instrumentations. Werner *et al.* also studied the Raman scattering peaks of the cinnabar phase of HgS as a function of pressure and observed that some of the Raman peaks disappear with increasing pressure. The disappearance of these Raman peaks was attributed to the increasing absorption of the sample at the laser frequency instead of to the phase-II-to-phase-III transition. The remaining Raman peaks may possibly also come from the residual phase II at that pressure due to the sluggishness of the transition.

Since the first two diffraction peaks of the new phase of HgSe appeared at both high- and low-energy sides of the NaCl (200) peak as shown in Fig. 4(a), it is natural to think that phase IV of HgSe may have a face-centered orthorhombic structure similar to the GaAs/InSb high-pressure phase.<sup>25,26</sup> In this kind of phase transition, the (200) peak of the cubic phase splits into the (200), (020), and (002) peaks of the orthorhombic phase. By the same token, the NaCl (220) peak will split into (220), (202), and (022) peaks. The calculated  $d$  spacings of (200), (020), and (002) peaks, however, do not agree with the observed spacings.

Another possible candidate for phase IV is a hexagonal crystal structure. Following the series of the diffraction pattern in Fig. 4, we found that the first peak ( $A$ ) has a  $d$  spacing very close to that of the NaCl (111) peak. The intensity of this peak first decreased and then slightly increased as the pressure was increased. Because the NaCl (111) phase is the closest packed plane of a face-centered cubic lattice, this  $d$  spacing would have to correspond to (002) planes of a hexagonal lattice. If this is the case, the next diffraction peak would correspond to the (101) planes (peak  $B$ ) of the hexagonal lattice. Although this index will give a reasonable value for the molar volume, again the calculated  $d$  spacings do not agree with the experimental  $d$  spacings for the other diffraction peaks. Since we have tried to fit all the  $d$  spacings to one crystal structure alone without success, we suggest that the diffraction peaks may come from the mixture of two coexisting phases. If we compare the major diffraction peaks [indexed as (200), (101), (220), and (211)] of HgSe with the diffraction pattern of HgTe phase IV, we find that they are very similar. Both can be indexed as bct lattice. The two extra peaks of HgSe (peaks  $A$  and  $B$ ) can then be indexed as the (002) and (101) of a hexagonal lattice. The recent calculations on the structural stability of III-V compounds as a function of pressure using the pseudopotential method show that the energy differences between some high-pressure phases are small and therefore it is quite possible that high-pressure phases may coexist.

There is another possible source of these two diffraction peaks, i.e., under high pressure, HgSe may disproportionate. This is impossible to verify at present because we do not have the equation of state of possible products such as Hg, Se, and Hg<sub>2</sub>Se. We note that these extra peaks are present in HgTe at pressures where they occur in HgSe.

Figure 3 shows the diffraction pattern of HgTe at 41 GPa. In addition to the diffraction peaks from phase IV,

TABLE IV. Analysis of the diffraction pattern of HgSe at 40.4 GPa, phase IV, body-centered-tetragonal lattice,  $a=5.112$  Å,  $c=2.721$  Å,  $\theta=6.518^\circ$ ,  $E_{\text{acc}}=5.0$  GeV,  $T=28^\circ\text{C}$ .

Index	$d_{\text{obs}}$	$d_{\text{cal}}$	$I_{\text{obs}}$	$I_{\text{cal}}^a$	$I_{\text{cal}}^b$
$A^c$	2.983		9		
$B^c$	2.761		6		
200	2.556	2.556	38	78	86
101	2.402	2.402	91	96	92
$C$	1.951		1		
220	1.767	1.807	147	147	147
211		1.750			
310	1.626	1.616	4	11	12
$D$	1.551		1		
301		1.444		24	23
002	1.370	1.361	11	1	6
$F$	1.323		1		
112		1.273			
400	1.270	1.278	1	47	37
321		1.256			
202	1.215	1.204	11	2	7
330		1.204			
420	1.139	1.142	4	4	4

<sup>a</sup>Basis: Hg(0,0,0), Te(0,  $\frac{1}{2}$ ,  $\frac{1}{4}$ )

<sup>b</sup>Basis: Hg(0,0,0), Te(0,  $\frac{1}{2}$ , 0)

<sup>c</sup>The origin of peaks  $A$  and  $B$  are discussed in the text. Very weak peaks  $C$ ,  $D$ , and  $F$  are not included in the calculation. Peak  $D$  is probably due to the remaining phase III, while the origin of  $C$  and  $F$  are unclear. The reliability factor  $R$  is 0.54 and 0.48 for the two cases a and b, respectively.

there are three extra peaks of  $d$  spacings of 2.361, 2.085, and 1.469 Å, respectively. The structural transition from the NaCl structure to the CsCl structure was suggested by the ionic radius ratio rule<sup>27</sup> and Jayaraman *et al.*<sup>8</sup> The lattice parameter determined from the three peaks indexed as (110), (111), and (210), of the CsCl structure are 3.339, 3.611, and 3.284 Å and the deviation suggests this is not a CsCl phase and perhaps it is a distorted CsCl phase. The origin of these three peaks in HgTe is different from the two extra peaks in HgSe mentioned above because these three diffraction peaks have  $d$  spacings smaller than those of (200) and (101) peaks of phase IV while the two extra peaks mentioned previously have spacings larger than (200) and (101) peaks of phase IV. The two extra peaks,  $A$  and  $B$ , in HgSe start to appear during phase-III-to-phase-IV transition while these three peaks in HgTe start to appear at a pressure far above the

phase—III—to—phase-IV transition pressure.

The phase transition from the cinnabar structure to the NaCl structure may be a second-order transition. Figure 6 shows the cinnabar crystal structure. This structure is built up of infinite spiral chains  $(-S-Hg-)_n$ , running parallel to the  $C$  axis of the hexagonal unit cell as shown in Fig. 6(a). Figure 6(b) shows the other view of the cinnabar structure which is obviously a distorted NaCl crystal structure.<sup>28</sup> Because the cinnabar structure transforms into the NaCl structure through the gradual merging of the diffraction peaks as a function of pressure, we propose that this phase transition is a second-order transition. This phase transition is accomplished by the adjustment of the bond length and the bond angle when it transforms gradually from  $sp$  covalent bonding to six coordinated bonding.

Before discussing the volume change of the mercury chalcogenides during a phase transition, it is instructive to examine the anomaly of the lattice parameter of mercury chalcogenides at atmospheric pressure. For the Zn and Cd chalcogenides, this lattice parameter can be obtained by adding the covalent radii of its constituents. Although the covalent radius of Hg is larger than that of Cd, the observed lattice constant of HgTe is less than that of CdTe and the lattice constant of HgSe is the same as that of CdSe.<sup>29</sup> In other words, there is a reduction of the observed lattice constant in mercury chalcogenides which results from the compression of the crystal from the density expected on the basis of the covalent radii. This contraction is similar to the so-called "lanthanide contraction."<sup>30</sup> The "uncompressed" lattice parameter (the sum of the covalent radii) of HgTe, HgSe, and HgS are 6.621, 6.203, and 5.977 Å, respectively, as compared with the "compressed" (observed) values of 6.429, 6.084, and 5.852 Å, respectively.

According to Van Vechten's empirical relationship, the percentage volume change for a zinc-blende—to- $\beta$ -Sn transition in element-IV solids and III-V compounds ranges from 21% to 15% depending on the ionicity factor defined by Philips and VanVechten.<sup>31</sup> However, there is no direct comparison between mercury chalcogenides and these compounds because, first, as pointed out before, there is the "contraction" of these compounds at formation and second, there are intermediate phases (the cinnabar and the NaCl phase) present between the zinc-blende and the body-centered tetragonal [ $\beta$ -Sn]-like phase in mercury chalcogenides.

In HgSe, when the phase transition from phase III to phase IV occurs, the new diffraction peaks from phase IV are first observed at 28.3 GPa (the equilibrium transition pressure is probably lower) and the intensities of the phase-IV peaks increased while the intensities of the phase-III peaks decrease as the pressure is increased. The molar volumes of phase III and phase IV calculated at 30.4 GPa where both phases are present are  $22.17 \pm 0.15$  and  $22.48 \pm 0.15$  cm<sup>3</sup>, respectively. In other words, the density of the lower-pressure phase may be higher than the density of the high-pressure phase at the same pressure. For HgTe, the molar volumes of phase III and phase IV calculated at 14.8 GPa where both phases are present are  $28.92 \pm 0.20$  and  $29.63 \pm 0.20$  cm<sup>3</sup>, respectively.

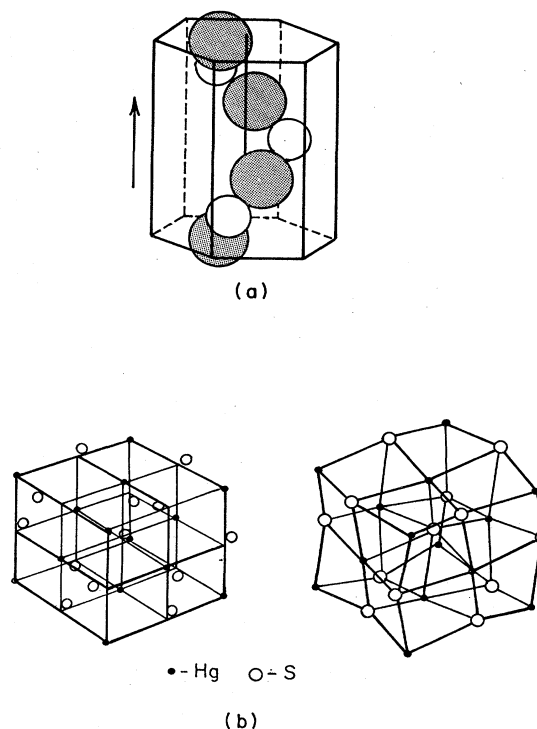


FIG. 6. Cinnabar crystal structure: (a) showing  $-Hg-S-$  spirals; (b) showing relation to NaCl structure.

The density of the persisting low-pressure phase may exceed that of the high-pressure phase at pressures substantially above the equilibrium transition pressure, if there is no volume change at the equilibrium transition pressure (a second-order phase transition) and the equation of state of the high-pressure phase is harder than that of the low-pressure phase. Note here that the pressures of 30.4 and 14.8 GPa are well beyond the transition pressure. This small amount of decrease in the density may explain the small increase in resistivity when the phase-III—to—phase-IV transition occurred in HgTe.<sup>11</sup> The resistivity versus pressure measurement for HgSe up to this pressure is not yet available. The fact that the density of the higher-pressure phase is less than the extrapolation of the density of the low-pressure phase has also been reported in CdS when it transforms from the NaCl structure to the KCN low-temperature structure.<sup>32</sup>

The only other IIB-VI compound that has been studied under high pressure above 20 GPa is CdS.<sup>32</sup> CdS transforms from its initial wurtzite structure to the NaCl structure at around 3 GPa. X-ray diffraction studies show that the NaCl structure is stable up to around 50 GPa. New diffraction lines started to appear at about 50 GPa and were indexed as the low-temperature KCN structure (orthorhombic, space group  $Pmmm$ ). Visual observations under a microscope indicate that the new high-pressure phase is still semiconducting instead of metallic, which may be due to the very small volume change (0.8%) at the transition.<sup>32</sup> Our results show that the NaCl phase of the mercury chalcogenides does not transform to this KCN structure under high pressure to 40 GPa.

It was concluded that phase IV of HgSe and HgTe has

a bct lattice by comparing the observed and calculated  $d$  spacings. In an attempt to determine the space group of this phase IV, the calculated relative intensities, assuming a bct lattice with a first basis Hg (0,0,0), Se/Te ( $0, \frac{1}{2}, \frac{1}{4}$ ) and a second basis Hg (0,0,0), Se/Te ( $0, \frac{1}{2}, 0$ ), are listed in columns 5 and 6 of Tables II and IV. It is possible that the actual position of the Se/Te atom is at ( $0, \frac{1}{2}, z$ ) where  $0 \leq z \leq \frac{1}{4}$ ; however  $z=0$  fits best.

For HgTe, there are no extra experimental lines and there are no major discrepancies with the  $z=0$  case, but the reliability factor ( $R=0.33$ ) is not as good as for phase III ( $R=0.13$ ). It is possible that texturing and nonhydrostaticity at the higher pressure associated with phase IV are responsible for the poorer  $R$  factor. The agreement is less good for HgSe. We note that the space group of phase IV of HgSe and HgTe is certainly different from the high-pressure  $\beta$ -Sn phase of GaP and InSb (Refs. 25 and 26, respectively) (in which the constituent elements are randomly distributed on the latter sites) because of the presence of (310), (002), and (202) diffraction peaks in HgSe and HgTe.

It has been pointed out that the core electrons contribute the major part of the total energy of the crystal but have little effect on the lattice parameter other than to screen the nuclear charge.<sup>17</sup> In the case of mercury compounds, there are  $4f$  electrons present. The effect of  $4f$  electrons can be seen by observing the unique properties (contraction) of mercury chalcogenides compared with its zinc and cadmium counterparts as mentioned previously. A first-principles band-structure calculation on these compounds would be valuable in understanding the contribution of the  $4f$  electrons in determining the band structure and crystal energy in compounds formed by elements with  $4f$  electrons. These results provide guidance for theoretical first-principles total-energy calculations.

## VI. CONCLUSIONS

In summary, we have made x-ray diffraction studies of mercury chalcogenides including HgS, HgSe, and HgTe to 40 GPa by energy-dispersive x-ray diffraction using CHESS. The results can be summarized as follows.

(1) The high-pressure phase-transition sequence can

be described by the following: zinc-blende—cinnabar—NaCl—body-centered tetragonal.

(2) Phase III of the mercury chalcogenides is determined to have the NaCl structure. The agreement between the measured and the calculated relative intensities is excellent.

(3) Phase IV of HgTe is a body-centered-tetragonal lattice with space group  $I\bar{4}m2$ . This structure is a body-centered-tetragonal lattice with a basis: Hg(0,0,0) and Se Te ( $0, \frac{1}{2}, z$ ). For the case  $z=\frac{1}{4}$ , this is an analog of the  $\beta$ -Sn structure in the same sense as the zinc-blende structure is of the diamond structure. The reliability factor is best for the  $z=0$  case. There are no important discrepancies in the case of HgTe. Texturing in the noncubic phase along with nonhydrostaticity at the pressures at which phase IV exist are probably responsible for the reliability factor being poorer for the bct structure of phase IV than for the NaCl structure of phase III.

(4) It is proposed that the diffraction pattern of phase IV of HgSe has the same structure as for HgTe although the agreement is not as good and there are some unexplained discrepancies.

(5) A new high-pressure phase V of HgTe was observed and may possibly be a distorted CsCl structure.

(6) The zinc blende to NaCl to bct phase transition is similar to that in zinc and cadmium chalcogenides except for the presence of the intermediate cinnabar phase in mercury chalcogenides.

(7) The difference in the phase transition sequence in mercury chalcogenides and zinc or cadmium chalcogenides may be attributed to the presence of  $4f$  electrons.

## ACKNOWLEDGMENTS

We acknowledge the National Aeronautics and Space Administration and the National Science Foundation through the Cornell Materials Science Center for support of this work. We also acknowledge the National Science Foundation for support on Grant No. 83-05798. Also, helpful discussions with A. Jayaraman are appreciated. Finally we would like to thank W. A. Bassett for use of equipment and the staff of the Cornell High Energy Synchrotron Source for their help.

<sup>1</sup>S. Minomura and H. G. Drickamer, *J. Phys. Chem. Solids* **23**, 451 (1962).

<sup>2</sup>G. A. Samara and H. G. Drickamer, *J. Phys. Chem. Solids* **23**, 457 (1962).

<sup>3</sup>N. B. Owen, P. L. Smith, J. E. Martin, and A. J. Wright, *J. Phys. Chem. Solids* **24**, 1519 (1963).

<sup>4</sup>P. L. Smith and J. E. Martin, *Phys. Lett.* **19**, 541 (1964).

<sup>5</sup>A. Onodera, *Rev. Phys. Chem. Jpn.* **34**, 64 (1969).

<sup>6</sup>A. Ohtani, M. Motobayashi, and A. Onodera, *Phys. Lett.* **75A**, 435 (1980).

<sup>7</sup>J. S. Kasper and M. Brandhorst, *J. Chem. Phys.* **41**, 3768 (1964).

<sup>8</sup>A. Jayaraman, W. Klement, Jr., and G. C. Kennedy, *Phys. Rev.* **130**, 2277 (1963).

<sup>9</sup>A. N. Mariano and E. D. Warekoi, *Science* **142**, 672 (1964).

<sup>10</sup>A. Kafalas, H. C. Gatos, M. C. Lavine, and M. D. Banus, *J. Phys. Chem. Solids* **23**, 1541 (1962).

<sup>11</sup>A. Onodera, A. Ohtani, M. Motobayashi, T. Seike, O. Shimomura, and O. Fukunaga, in *Proceedings of the 8th AIRAPT Conference, Uppsala, Sweden, 1981*, edited by C. M. Backman, T. Johannisson, and L. Tegner (Arkitektkopia, Uppsala, 1982), Vol. 1, p. 321.

<sup>12</sup>B. Ray, *II-VI Compounds* (Pergamon, New York, 1969), Chap. 7, p. 229.

<sup>13</sup>T. Huang and A. L. Ruoff, *J. Phys.* **54**, 5459 (1983).

<sup>14</sup>T. Huang and A. L. Ruoff, *Phys. Rev. B* **27**, 7811 (1983).

<sup>15</sup>T. Huang and A. L. Ruoff, *Phys. Status Solidi* **77**, K193 (1983).

<sup>16</sup>A. Werner, H. D. Hochheimer, K. Strossner, and A. Jayaraman, *Phys. Rev. B* **28**, 3330 (1983).

- <sup>17</sup>J. A. Van Vechten, *Phys. Rev. B* **7**, 1479 (1973).
- <sup>18</sup>J. C. Philips, *Bonds and Bands in Semiconductors* (Academic, New York, 1973), Chap. 8, p. 201.
- <sup>19</sup>S. C. Yu, I. L. Spain, and E. F. Skelton, *Solid State Commun.* **25**, 49 (1978).
- <sup>20</sup>A. L. Ruoff and M. Baublitz, Jr., Proceedings of the International Symposium on the Physics of Solids Under High Pressure, Bad Honnef, Germany (unpublished).
- <sup>21</sup>M. T. Yin and M. L. Cohen, *Phys. Rev. B* **26**, 5668 (1982).
- <sup>22</sup>S. Froyen and M. L. Cohen, *Phys. Rev. B* **28**, 3258 (1983).
- <sup>23</sup>G. J. Piermarini, S. Block, J. D. Barnett, and R. A. Forman, *J. Appl. Phys.* **46**, 2774 (1975).
- <sup>24</sup>G. J. Piermarini, S. Block, and J. D. Barnett, *Rev. Sci. Instrum.* **44**, 1 (1973).
- <sup>25</sup>M. Baublitz, Jr. and A. L. Ruoff, *J. Appl. Phys.* **53**, 6179 (1982).
- <sup>26</sup>M. Baublitz, Jr. and A. L. Ruoff, *J. Appl. Phys.* **54**, 2109 (1983).
- <sup>27</sup>N. W. Ashcroft and N. D. Mermin, *Solid State Physics* (Holt, Rinehart and Winston, New York, 1976), Chap. 19, p. 383.
- <sup>28</sup>N. Kh. Abrikosov, V. G. Bankira, L. V. Portskaya, and L. E. Shelimva, *Semiconducting II-VI, IV-VI, and V-VI Compounds* (Plenum, New York, 1960), Chap. 4.
- <sup>29</sup>J. C. Philips and J. A. Van Vechten, *Phys. Rev. B* **2**, 2147 (1970).
- <sup>30</sup>C. Kittel, *Introduction of Solid State Physics*, 5th ed. (Wiley, New York, 1976), Chap. 14, p. 442.
- <sup>31</sup>J. C. Philips and J. A. Van Vechten, *Phys. Rev. B* **2**, 2167 (1970).
- <sup>32</sup>T. Suzuki, T. Yagi, S. Akimoto, T. Kawamura, S. Toyoda, and S. Endo, *J. Appl. Phys.* **54**, 748 (1983).